of social behavior exist between the four species (*3*). This is not surprising, since the morphs are only expressions of the physiological and behavioral differences between castes. The more discontinuous the visible variation between queen and workers, the more complete is the division of labor and the ovarian inhibition of the workers. Suppression of males in the early broods is associated with the higher levels of social behavior; the summer brood of *A. striata* has as many males as females, while that of *E. cinctipes* has no males at all (*5*).

Determination of caste was once thought to be genetic, but female eggs have proved to be all alike in bees, wasps, and termites that have been studied so far. Plasticity within individuals rather than differences between them are transmitted genetically in social insects, and only the quality or quantity of food seems to influence the immature insect (*6*). The mechanism of caste determination is best known in honeybees, where the food of larvae (the protein and fat that comes from glands of adult workers) determines the fate of a diploid egg. A critical point is reached about the 3rd day in the larva's life, after which time determination can be only partially reversed (*7*). Similar processes are probably at work in highly evolved ant and wasp societies in which progressive feeding by trophallaxis is common. The more-primitive societies of halictine and some bumblebees feed their brood by mass provisioning, that is, food for the complete development of a new bee is supplied before the larva begins to feed. The physiological plasticity of Hymenoptera (*8*) allows completion of development on very small rations, and this trait must have favored the evolution of a subnutritional variant (worker). Production of such a caste is "cheaper" and also adaptive, since foraging queens spend less time away from the nest and thereby reduce the opportunities of predators and parasitoids.

Exchange of food (trophallaxis) has never been observed in halictine bees, and the lack of morphological specialization in the female castes makes it unlikely that there is a glandular mechanism of caste determination. There is a direct relation between the quantity of food provided and the size of the developing bee, at least in *E. cinctipes* (Fig. 2). Agreement between the two curves (wing length and weight of provisions) is really much closer than Fig. 2 suggests, because pollen measurements of the early summer phase have been included. Pollen balls at that stage are small (the workers apparently need some time to reach optimum proficiency in foraging), and the prevailing protandry in social species destines them for consumption by males.

With species like *H. ligatus*, which show gradual increase in the average size of workers produced during the summer, the amount of provisions tends to increase in the cells as more workers become available for field duties. No abrupt increase in the size of pollen balls was noted in these species before fall; this fact explains the presence of overwintered females of intermediate sizes in pleometrotic (of more than one female) associations in the following spring (*3*). An even smaller difference is found between the pollen balls of the spring and summer phases of *A. striata*, a species having small queens scarcely larger than the smallest workers, and large workers approaching the size of the biggest queens (Fig. 1).

G. Knerer*
C. E. Atwood
Department of Zoology, University of Toronto, Toronto, Ontario

References and Notes

1. O. W. Richards, *Symp. Roy. Entomol. Soc. London* **1**, 1 (1961).
2. J. H. Law, E. O. Wilson, J. A. McCloskey, *Science* **149**, 544 (1965).
3. G. Knerer and C. E. Atwood, *Animal Behav.*, in press.
4. C. Plateaux-Quénu, *Ann. Biol.* **35**, 325 (1959).
5. G. Knerer, dissertation, Univ. of Toronto, 1965.
6. M. V. Brian, *Symp. Zool. Soc. London* **14**, 28 (1965).
7. C. R. Ribbands, *The Behaviour and Social Life of Honeybees* (Bee Research Assoc., London, 1953), p. 246.
8. A. Popovici-Baznosanu, *Compt. Rend. Soc. Biol. Paris* **69**, 480 (1910).
9. Supported by the National Research Council of Canada. We thank J. Simpson for help with the manuscript.

* Present address: Bee Department, Rothamsted Experimental Station, Harpenden, England.

26 February 1966

Insect Aerodynamics: Vertical Sustaining Force in Near-Hovering Flight

Abstract. *The source of vertical sustaining force for large insects capable of near-hovering flight is unclear. Induced velocities of a simulation of the insect* Melolontha vulgaris *in forward flight were measured with a hot-wire anemometer. The results were negative with respect to the drag concept of vertical force, but provided certain support for the circulation concept. Unsteady effects (the effects of variant air velocity) proved significant.*

Flight of birds (*1*) and large insects (*2*) is generally described by means of strip-integration, quasi-steady circulation techniques. However, as flying insects approach the "hovering condition"—that is, as the ratio of forward speed to flapping speed becomes small—requisite lift coefficients become surprisingly large (*3*). Because insect-flight Reynolds numbers (Re) range from approximately 3 to 5000, a range unfavorable (*4*) for the development of large lift coefficients, other possible explanations of a vertical sustaining force have maintained currency.

One such possibility is the drag concept (*5*), in which the difference between downstroke and upstroke drag is deemed the prime source of support. This view has been advocated particularly for the smallest of insects (*6*), moving at Re so low (≤ 10) that air is experienced as a largely viscous medium; but at higher Re the validity of this concept is uncertain.

Another possibility is that of virtual-mass effects (*3*): As the wing accelerates the apparent inertia is increased by the mass of air (induced mass) that is influenced by the motion of the wing; for example, in the case of a small acceleration normal to a nominal flight path, the induced mass encompasses the cylinder of air whose diameter equals the wing chord (*7*). As the apparent inertia of but a portion of this mass, the boundary layer, has been deemed significant to the wing loading of insects (*8*), it is conceivable that induced-mass acceleration may produce usefully large, transient, lift forces.

A large insect exhibiting near-hovering characteristics was chosen for examination of these possibilities. *Melolontha vulgaris*, a beetle, has size and velocity such that the airflow Re falls well outside the Stokes drag regime. If the vertical sustaining force arises largely from circulation effects, it has been calculated (*3*) that a mean lift coefficient of about 2.0 is required on the downstroke. By the standard of experience with propellers and helicopters, which operate at an Re more favorable for the generation of large lift coefficients, a value of 2.0 is large.

To test the significance of the various concepts of vertical force, instantaneous induced velocity as a function of azimuth has been measured for a simulation of the forward flight of *M. vulgaris*; the simulation was deemed preferable to a real insect (*9*) for many weeks of testing under fixed conditions, and a mechanical device simplifies parametric variation. To minimize error in simulation, high-speed motion pictures of the insect in flight (*10*) were analyzed frame by frame by the techniques of descriptive geometry; true blade incidence at the $0.7R$ (R is wing length) station, instantaneous flapping velocity, and tip-plane angle with respect to direction of flight were determined. Additional measurements were obtained directly from specimens (*11*).

These results were incorporated in a full-scale model (Fig. 1). Incidence was changed automatically by a set of weights so mounted on the wing root as to produce an inertial torque when the wing experienced acceleration in the flapping plane; the effect was to alter incidence sharply at the beginnings and ends of periods of both downstroke and upstroke. Stops machined into the housing were set for desired limits of upstroke and downstroke. The wing proper was fashioned with music-wire leading and trailing edges; cellophane tape, covering both upper and lower sides of the wire loop, served as the wing surface.

To introduce appropriate interaction effects occurring between opposing wings into the single-wing model, a solid image plane was placed in a position corresponding to the insect's vertical plane of symmetry. A small cutout permitted passage of the balance weight.

Forward speed was duplicated with a miniature, open-throat, open-circuit, wind tunnel; low level of turbulence and fair velocity profile (± 5 percent) were obtained by passing the air through a series of air-conditioning filters.

The simulated flight (see Table 1) departs from the true condition in three respects: (i) the effect of the elytra (hard wing covers) is ignored; as these are relatively small in area and nearly fixed in incidence, and have low flapping speed, they are viewed as contributing little to the total vertical force; (ii) the maximum rate of change of incidence of the model wing is considerably less than that of the insect—for example, the change of incidence in an insect at the start of a downstroke is largely complete within 5 degrees of flapping motion, while the corresponding flapping motion in the model is 20 degrees; consequently the angle of attack at the beginning and end of each stroke is not truly duplicated; (iii) no attempt was made to simulate wing twist or section camber; both factors, small at all times in the downstroke, were assumed to be of second-order significance.

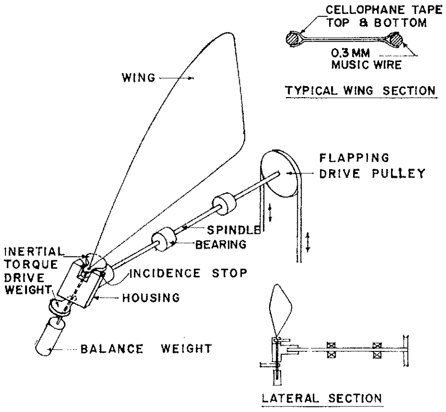

Fig. 1. Mechanism simulating flight of *Melolontha vulgaris*.

Induced velocities were measured with a commercial hot-wire anemometer (*12*) employing the high-frequency-response, constant-temperature concept. Velocity calibration was effected by attaching the sensor to a pendulum and swinging the package through stagnant air; pendulum velocity was measured from interruptions of light beams directed at two photomultiplier stations. The time constant of the entire anemometer system in stagnant-air conditions was measured at 0.45 msec with a built-in calibration system. This value may be viewed as conservative; at any induced velocity greater than zero the time constant is smaller.

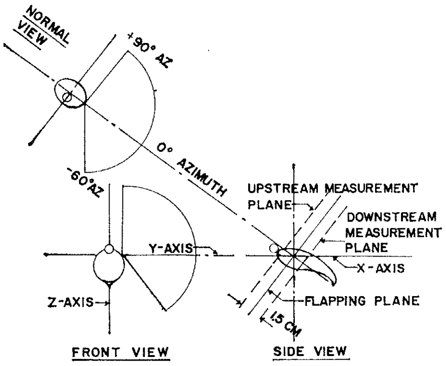

Fig. 2. Insect-flight reference axes; outline and attitude of the insect are not to scale.

Hot-wire velocities were presented on a conventional oscilloscope equipped with an external trigger circuit. The trigger was intermittently actuated by a solid-state photocell viewing a miniature lamp through a chopper attached to the main flapping drive; the velocity trace was thus initiated whenever the wing arrived at its uppermost position. Trigger precision was reduced by long-term drift characteristics to within 1.5 msec, as checked against a photomultiplier standard, but short-term error was negligible.

In operation, the hot-wire probe was positioned everywhere at the $0.7R$ point and moved within upstream and downstroke planes, adjacent to and parallel with the flapping plane (Fig. 2). Reference axes consisted of the true vertical (Z), the horizontal (X) lying in the plane of insect symmetry and perpendicular to the vertical, and the lateral (Y) perpendicular to both horizontal and vertical axes. As the direction of airflow was of interest, the probe, always lying in a vertical plane (Z–X), was oriented in each of nine different attitudes at every position sampled; by comparison of the nine values at a given elapsed time (percentage of the cycle), a single pair representing maximum and minimum values was selected; all others were discarded. The maximum value represents the condition in which the flow is most nearly perpendicular to the hot wire; the minimum, the condition in which the flow is most nearly parallel. The scalar value of the velocity vector is that of the maximum, directed at an angle given by the minimum-value attitude. Implicit is the assumption, reinforced by the presence of the image plane, that all significant velocities lie in the Z–X plane.

A typical raw-data record (Fig. 3), depicting upstream airflow, consists of four superimposed traces, each depicting more than two complete cycles. Note that scatter is small, indicating that the event is cyclic and the level of turbulence is low. A corresponding downstream record at the same settings demonstrates a larger scatter and slight turbulence.

Components of induced velocity, time-averaged over a complete cycle at given azimuth locations, are shown in Figs. 4 and 5. The time-averaged results permit application of the quasi-steady momentum theorem for determination of the vertical force gradient: the appropriate expression is

$$\frac{dF_z}{dr} = \rho 2\pi r \frac{A}{180} V_{rd} \times \left[\left(V_f + \frac{V_{hu} + V_{hd}}{2}\right)\sin\beta + \left(\frac{V_{ru} + V_{rd}}{2}\right)\cos\beta\right] \quad (1)$$

where ρ is mass density air (g·cm^{-4}/sec^2), r is local radius [0.7R (cm)], A is total effective azimuth (degrees), F_Z is vertical force (g), V_{rd} is downstream vertical induced velocity (cm/sec), V_f is speed of forward flight (cm/sec), V_{hu} is upstream horizontal induced velocity (cm/sec), V_{hd} is downstream horizontal induced velocity (cm/sec), V_{ru} is upstream vertical induced velocity (cm/sec), and β is angle between flapping plane and horizontal (degrees).

Equation 1 is developed from the classic momentum equation relating force to the product of mass flow and total velocity change in a direction of interest. While the intervening manipulation is straightforward, the following should be noted: All velocities directed downward and rearward with respect to the insect are considered positive; all velocity terms are azimuth-averaged; quantity A is the angle through which airflow is influenced—a larger value than the stroke. The values measured for downstream induced velocity are assumed to be fully developed, and further conversion of pressure head to kinetic energy is considered negligible (this assumption is conservative).

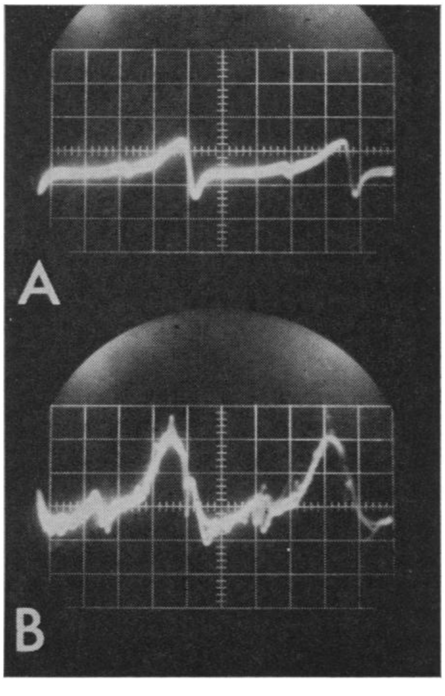

Fig. 3. Typical recordings of raw data on induced velocity. *A*, Upstream airflow at azimuth 0°; forward speed, 250 cm/sec; hot-wire attitude, + 30° from the horizontal. *B*, downstream airflow under identical conditions. Velocity scale, 173 cm/sec per box; time scale, 5 msec per box starting from the extreme right. The large pulse in both records corresponds to the downstroke.

To determine the compatibility of the vertical force gradient with that produced by circulation, use is made of the well-established propeller relation (*13*) between the force gradient at the 0.7R position and total force:

$$F_Z = 0.57R(dF_z/dr) \quad (2)$$

By combination of Eqs. 1 and 2 and insertion of appropriate values from Table 1 and Figs. 4 and 5, F_Z is 1.06 g, whereas the insect weighs 0.96 g; the difference represents errors in modeling, experimental errors, and the use, in gradient expressions, of the product of means rather than the mean of the products. These terms are not perfectly commutative; an error of several percent is introduced.

The horizontal force F_X represents the net thrust developed through wing action, that is, the force required to balance the drag of the remainder of the insect; it is obtained by equating force to the product of mass flow and velocity change in the X direction; this change is obtained experimentally from the difference $(V_f + V_{hd}) - (V_f)$. When V_f is large compared with V_{hd}, as in this work, a small error in the measurement of each bracketed term produces a large difference error. Therefore V_{hd} values, and F_X determinations based on them, are insufficiently accurate for quantitative purposes; thus the value of F_X in the simulated condition, determined as 0.34 g, indicates only the order of magnitude. The large tare problem does not arise in vertical force measurements; vertical tare is zero, and the mass-flow term involving V_{hd} exerts a second-order influence; consequently all quantitative efforts were confined to vertical force.

The significance of the vertical-force result given above stems from the means of determination. A reasonable estimate of the insect's vertical sustaining force was obtained when the measured change of momentum gradient, at a salient radial location, was treated as one arising from circulation. That is, the mean induced velocities experienced at the test location are those to be expected from circulation considerations, despite the large lift coefficients involved. While conceivably the agreement may be fortuitous, it may be said that all evidence yielded by this experiment supports the circulation concept.

Table 1. Test conditions for simulated flight of *Melolontha vulgaris*. Re, Reynolds number.

Conditions	
Single-wing area	1.8 cm^2
Wing length (R)	2.8 cm
Wing chord (at 0.7R)	0.85 cm
Flapping rate	46 cy/sec
Forward flight speed	250 cm/sec
Mean downstroke Re (at 0.7R)	3100
Mean tip advance ratio	0.35
Mid-downstroke incidence (at 0.7R)	32 deg
Mid-upstroke incidence (at 0.7R)	9 deg
Stroke amplitude	144 deg
Tip-plane angle with X-axis	60 deg

Further, I conclude that the lifting process results from increase in the downward vertical momentum of air passing through the flapping plane. This is significant, for, if the vertical force were derived largely from downstroke drag, the downstream vertical momentum would be lower than the corre-

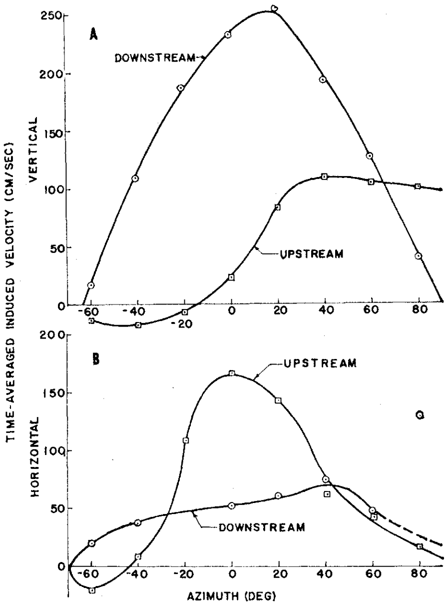

Fig. 4. *A*, Variation of the vertical component, of time-averaged induced velocity, with azimuth in simulated flight; positive velocity values are downward with respect to the insect. *B*, Variation of the horizontal component, of time-averaged induced velocity, with azimuth in simulated flight; positive velocity values are rearward with respect to the insect.

sponding flapping-plane vertical momentum; the reverse is true (Fig. 4).

The secondary importance of drag is corroborated by the low turbulence level of the downstream recordings. Should the basic vertical force stem from drag, a large drag coefficient would be necessary—one equivalent to a full stall throughout the downstroke. Comparison of the downstream turbulence levels of the wing flapping at a deliberately stalled attitude with those obtained at proper incidence indicates that, in a simulated condition, the stall or near-stall region is small, covering less than 20 percent of the total effective azimuth; it follows that the average drag coefficient must be small. As the findings regarding both momentum and turbulence oppose the drag hypothesis of vertical force, the hypothesis appears to be an unlikely mechanism.

Unsteady effects, significant to both circulatory and virtual mass forces, were evaluated through a series of tests in which the unsteady quality was reduced in steps. Noting that the greatest vertical force is sensed at mid-downstroke azimuth, I chose as a performance index the vertical impulse experienced by air moving through a unit area located at this position in the course of a single downstroke. This value was obtained by integrating the instantaneous vertical force, with respect to time, as the wing swept the hot-wire sensor located at the $0.7R$-radius midstroke azimuth; the appropriate value for a simulated flight is 3.32×10^{-3} g·sec/cm^2.

The wing was then arranged to represent near-steady conditions. Constant tangential velocity was obtained by removing the oscillating drive and image plane and substituting a continuous drive; the resultant configuration may be described as a single-bladed propeller operating with its axis inclined at a large angle of pitch. Values of fixed-blade incidence and tangential velocity were set equal to those developed by the simulated insect at mid-downstroke. The vertical-unit-area impulse imparted by the descending blade was determined at 1.67×10^{-3} g·sec/cm^2.

True steady-state conditions were then established by setting the wind tunnel axis normal to the propeller disc; wind speed was altered to the normal component of the above tests, but all other experimental conditions were unchanged. Vertical-unit-area impulse measured 1.19×10^{-3} g sec/cm^2.

These experiments do not support Jensen's (*14*) conclusions that insect flight in general may be treated as a sequence of stationary flow situations. It is apparent, from the unit-area-impulse results, that unsteady effects dominate simulated performance of *M. vulgaris*. Whether this influence is manifested through vigorous destalling (circulation concept) or virtual mass forces remains to be demonstrated.

LEON BENNETT

School of Engineering and Science,
New York University, University
Heights, Bronx 10453

References and Notes

1. G. T. Walker, *J. Roy. Aeron. Soc.* **29**, 590 (1925).
2. T. Weis-Fogh and M. Jensen, *Phil. Trans. Roy. Soc. London Ser. B.* **239**, 415 (1956).
3. M. F. M. Osborne, *J. Exp. Biol.* **28**, 232 (1951).
4. A. Thom and P. Swart, *J. Roy. Aeron. Soc.* **44**, 761 (1940).
5. A. Magnan, *Le Vol au Point Fixe* (Hermann, Paris, 1933), p. 7.
6. G. C. Horridge, *Nature* **178**, 1334 (1956).
7. R. L. Bisplinghoff, H. Ashley, R. L. Halfman, *Aeroelasticity* (Addison-Wesley, Cambridge, Mass., 1955), p. 263.
8. S. Vogel, *Nature* **193**, 1201 (1962).
9. A technique for measuring real-insect wake velocity is outlined in S. Vogel, *Proc. Intern. Congr. Entomol. 12th London 1964* (1965), p. 189.
10. A. Magnan, *Cinematographie jusqu'à 12,000 Vues par Seconde* (Hermann, Paris, 1932), p. 12; *Le Vol des Insectes* (Hermann, Paris, 1934), pl. 19, 20.
11. Generously supplied by the American Museum of Natural History.
12. Model CTA-2, Flow Corp., Cambridge, Mass.
13. W. F. Durand, *Aerodynamic Theory* (Dover, New York, 1963), vol. 4, p. 242.
14. M. Jensen, *Phil. Trans. Roy. Soc. London Ser. B.* **239**, 549 (1956).
15. I thank instrument maker Igor Sahajdakowski whose ingenuity made the model possible, graduate students Walter Lorell and M. Norman Schwartz for laboratory and theoretical efforts, and the NSF for support (GP-2568).

7 March 1966

Root Pressure and Leaf Water Potential

Abstract. *Measurements with thermocouple psychrometers were made of the water potentials of leaves from sunflower and pepper plants which had stood overnight in the dark in nutrient solutions containing carbowax. Similar measurements on the solutions showed that they had lower water potentials than the leaves, although the plants were measurably transpiring. Evidence that root pressure plays a part in this inversion of water potential gradient is presented.*

In studies of the movement of water through plants it is generally accepted that the gradient of water potential increases (negatively) from the soil, through the plant to the atmosphere, and that water (or in the final stage water vapor) flows passively down this gradient (*1*). The energy source for maintaining the gradient is the evaporative demand of the plant's aerial environment. If this view is correct, then leaf water potential must always be lower (more negative) than soil water potential, as long as the atmosphere is the final sink. I now report that, under certain conditions, leaf water potential may in fact be higher (less negative) than the water potential of the rooting medium, although the overall direction of flow is still into the atmosphere. Supplementary experiments suggest that root pressure may be responsible for this inversion of part of the water potential gradient.

Pepper (*Capsicum frutescens* L. 'Californian Wonder') and sunflower (*Helianthus annuus* L. 'Large Grey') plants were grown in the greenhouse in full strength Hoagland culture solution with iron supplied as sequestrene 138 Fe-chelate. When used for experiments the pepper plants were 2 to 3 months old, and the sunflower plants were about 6 weeks old. In the experiments, plants were transferred to a humidity- and temperature-controlled growth cabinet and kept in the dark for 8 to 12 hours prior to sampling. At the time of transfer, water potential of the culture solution (about −0.5 bar) was lowered further by the addition of varying amounts of carbowax (1540 or 4000) to give a range of water potentials of −3 to −10 bars. Cabinet temperature was 23°C and relative humidity high (90 percent) or low (30 percent). Leaf water potentials were measured with Spanner-type psychrometers and corrected for tissue respiration (*2*). Duplicate measurements of solution water potentials were made with Spanner or Richards and Ogata psychrometers, or both (*3*). Experiments of this type show (Table 1), that for pepper at high relative humidity, leaf water potential is always higher than that of the solution bathing the roots, even when the solution water potential is nearly −10 bars. At low relative humidity, this inverted gradient is less steep, but is still maintained in all cases except for the −10 bar solution. Similar inverted gradients are found at high relative humidity in sunflower plants grown in full strength Hoagland solution, but for sunflower